

Capability of constitutive models to simulate soils with different OCR using a single set of parameters

Václav Hájek*
David Mašín*
Jan Boháč*

**Faculty of Science, Charles University in Prague, Czech Republic*

correspondence to:

David Mašín

Charles University in Prague

Faculty of Science

Albertov 6, 128 43 Prague 2, Czech Republic

E-mail: masin@natur.cuni.cz

Tel: +420-2-2195 1552, Fax: +420-2-2195 1556

October 30, 2008

Technical Note accepted for publication in *Computers and Geotechnics*

Abstract

Incorporation of void ratio as a state variable into constitutive models allows, in principle, to use a single set of parameters for soils with different *OCRs*. Two sets of experimental data on reconstituted clays are used for evaluation of three constitutive models of different complexity (Modified Cam clay model, 3-SKH model, hypoplastic model for clays). Although all the models predict the influence of *OCR* correctly from the qualitative point of view, quantitative comparison using a suitable scalar error measure reveals merits and shortcomings of different models.

Keywords: clay; overconsolidation ratio; constitutive model; hypoplasticity; kinematic hardening.

1 Introduction

It has been recognised since the development of critical state soil mechanics in 1960's that realistic constitutive models should consider void ratio e as a state variable. This approach, in theory, allows to use a single set of material parameters to predict the behaviour of soils with a broad range of overconsolidation ratios (*OCRs*) and thus simplifies practical application of constitutive models. As a matter of fact, however, qualitatively correct predictions of the behaviour of soils with different *OCRs* based on a single set of material parameters do not necessarily imply satisfactory performance from the quantitative point of view. An engineer aiming to apply the constitutive model for solution of practical geotechnical problems should be aware of the range of *OCRs* for which a single set of material parameters may be used and design an experimental program accordingly. Also, the mean stress and *OCR* vary throughout the soil strata. If their influence is not predicted appropriately, different parameter sets must be used for different depth levels, which is not desirable.

To the knowledge of the authors, a detailed evaluation of constitutive models in this respect is missing throughout the geotechnical literature. To investigate predictive capabilities of currently available constitutive models, three models of different complexities based on different mathematical backgrounds have been evaluated using two sets of experimental data on reconstituted fine-grained soils at different *OCRs*. It is acknowledged that complete evaluation of the models for use in practical problems should consider a wide range of stress paths and loading conditions, preferably directional response of soil should be studied (see, e.g., [14, 5]). As such detailed experimental data for different *OCRs* are not available, the present evaluation focus on shear experiments performed under axisymmetric conditions in the triaxial apparatus.

Soil mechanics sign convention is used throughout this paper, i.e. compression stresses and strains are positive. All stresses are effective stresses in the sense of Terzaghi principle. The single element and finite element implementations of all the models considered is freely available [4].

2 Experimental data

Two sets of experimental data have been used throughout this study. The first is a comprehensive set of data on kaolin clay by Hattab and Hicher [6], which has been supplemented by purpose-made experiments on reconstituted kaolinitic-illitic clay in order to draw more general conclusions.

The experiments on kaolin clay have been described in detail in Reference [6]. They were conducted in a Bishop and Wesley triaxial apparatus with computer control, which made it possible to follow the constant effective mean stress p path with accuracy ± 1 kPa. The axial deformation has been recorded by means of external LVDT transducers and volumetric strains using GDS pressure controllers. The specimens of kaolin clay with Atterberg limits $w_L = 40\%$ and $w_P = 20\%$ were prepared in a consolidometer from a slurry at a water content of twice the liquid limit. The height of the samples was equal to their width (35 mm) and smooth end-plattens were used. The specimens were isotropically loaded up to the maximum preconsolidation pressure $p_0 = 1000$ kPa and then isotropically unloaded to the pressure $p = p_0/OCR$,

from which the shear tests at constant mean stress p followed. Altogether 12 shear experiments are reported, at $OCR = 1, 2.25, 2.5, 2.7, 3, 4, 5, 8, 10, 20$ and 50 , with stress paths shown in Fig. 1(a).

The soil for the second set of experiments was a kaolinitic-illitic clay from a Tertiary sedimentary basin near Ústí and Labem, Czech Republic, which is characterised by $w_L = 58 - 62\%$ and $I_P = 29 - 34\%$ [7]. Constant cell pressure drained triaxial tests have been performed in a triaxial cell using a load frame. Axial deformation has been measured externally by means of digital dial gauge, volumetric strains were recorded by GDS pressure controllers.

The soil from a rotary drill core was reconstituted in distilled water at a water content approximately $1.5 w_L$, transferred into a double drainage consolidometer and consolidated under vertical load of 70 kPa, which was enough to create specimens that could be handled and transferred into the triaxial apparatus. After removing from the consolidometer, the specimens were trimmed to a slenderness ratio $2:1$ ($D=38$ mm, $H=76$ mm) and set up in the triaxial cell. A radial drainage has been used in order to speed up the dissipation of pore pressures, while the bottom drainage was facilitated by rough end platens. Before testing, Skempton B-value has been measured in order to check saturation of the samples. A minimum value of 97% was required.

A similar test procedure to that of Hattab and Hicher [6] has been followed, i.e. the specimens were first isotropically consolidated to the mean stress $p_0 = 600$ kPa and then isotropically unloaded to $p = p_0/OCR$. Five different values of OCR have been applied, namely $OCR = 1, 1.5, 2, 4$ and 8 . From this state, strain-controlled drained triaxial tests have been conducted up to failure, at the rate of axial deformation of 0.001 mm/min. The stress paths are shown in Fig. 1(b). Due to the use of the rough end platens, the deformation tended to localise into shear bands in the post-peak regime, especially in the case of specimens tested at higher overconsolidation ratios. This rendered the large-strain data less reliable, it had however only little influence on the pre-peak states, which were in a particular scope of this study.

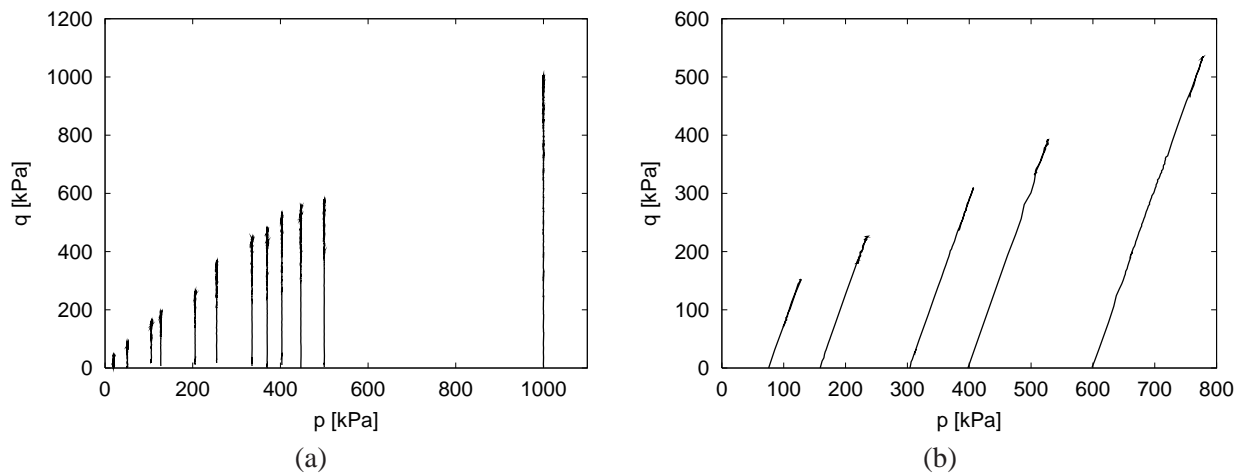


Figure 1: Stress paths of experiments used for evaluation of the models on kaolin clay by Hattab and Hicher [6] (a) and illitic clay (b).

3 Constitutive models and their parameters

Three constitutive models of different complexity and based on different mathematical backgrounds have been selected for evaluation presented in the paper. All of them are based on the critical state soil mechanics and as such it is implicitly assumed that consideration of void ratio (or, equivalently, preconsolidation pressure) as a state variable is sufficient to use a single set of material parameters for predicting the behaviour of soils with different $OCRs$.

The first model considered is a basic critical state soil mechanics model, *Modified Cam clay (CC)* [17]. This model has a number of well-known shortcomings, among which possibly the most important is an

elastic behaviour inside the yield surface and overprediction of peak friction angles φ_p of overconsolidated soils. However, as this model is still widely used in practice it provides a valuable reference for the two more advanced models considered. In this work a version with Butterfield's [3] compression law is used, mainly due to the simplified comparison with the two other models, which use the same compression law. Therefore, the isotropic virgin compression line reads

$$\ln(1 + e) = N - \lambda^* \ln(p/p_r) \quad (1)$$

with parameters N and λ^* and a reference stress $p_r = 1$ kPa. The slope of the isotropic unloading line is controlled by the parameter κ^* , a constant shear modulus G is assumed inside the yield surface and the stress ratio $\eta = q/p$ at critical state (where q is shear stress and p is mean stress) is equal to the parameter M .

The second model, *three surface kinematic hardening model (3SKH)* by Stallebrass and Taylor [19], is an advanced example of the kinematic hardening plasticity models for soils [15]. The model represents an evolution of the CC model and of the two surface kinematic hardening model by Al Tabbaa and Muir Wood [1]. With respect to the model by Al Tabbaa and Muir Wood [1], two kinematic surfaces in the stress space (named yield surface and history surface) improve predictions in the small strain range and enable the effects of recent stress history [2] to be modelled. Since the hardening modulus depends on the distance from the outer bounding surface (of the same shape as the yield surface of the CC model), the 3SKH model predicts the non-linear behaviour inside the bounding surface and thus it does not suffer from the two main shortcomings of the CC model. Sketch of the three characteristic surfaces of the 3SKH model is in Fig. 2.

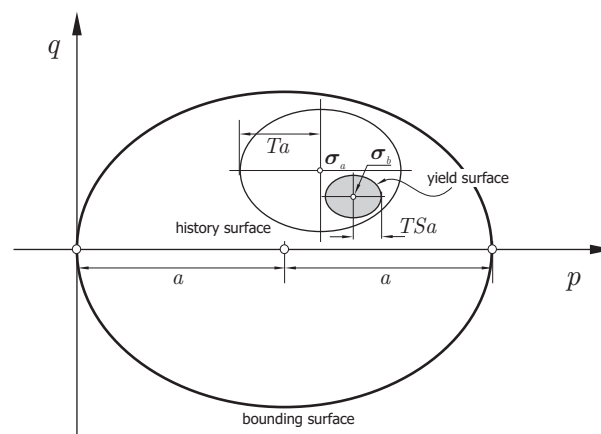


Figure 2: Characteristic surfaces of the 3-SKH model, from Mašín et al. [14].

Four of the parameters of the 3SKH model, namely N , λ^* , κ^* and M , have the same meaning as the parameters of the considered version of the CC model. The shear modulus inside the elastic range G is calculated from an equation by Viggiani and Atkinson [20]

$$\frac{G}{p_r} = A \left(\frac{p}{p_r} \right)^n OCR^m \quad (2)$$

with parameters A , n and m . The parameters T and S characterise the relative sizes of the kinematic surfaces, as demonstrated in Fig. 2 (if we denote the size of the bounding surface $2a$, then the sizes of history and yield surfaces are equal to $2Ta$ and $2TSa$ respectively). The last parameter, ψ , is an exponent that controls the influence of the distance of the current stress state from the bounding surface on the hardening modulus, and therefore it controls the rate of decay of stiffness as the state moves towards bounding surface (as demonstrated later in the text, e.g. Fig. 9).

The last model tested is based on a mathematically different approach – hypoplasticity. A *hypoplastic constitutive model for clays (HC)* was proposed by Mašín [11] and investigated further by Mašín and Herle [13], who have shown that the model predicts the state boundary surface (defined as a boundary of all

possible states in the stress vs. void ratio space), although it is not explicitly incorporated in its mathematical formulation. The model combines the mathematical formulation of hypoplastic models (e.g., [9, 21, 16, 8]) with the basic principles of the critical state soil mechanics, and therefore the influence of OCR is predicted in a qualitatively similar way to the 3SKH and CC models. Similarly to the 3SKH model, the hypoplastic model predicts non-linear behaviour inside the state boundary surface, and therefore it does not suffer from shortcomings of the CC model.

The model requires five parameters with a similar physical interpretation as parameters of the CC model. N and λ^* are coefficients in the Butterfield's [3] compression law (1), κ^* controls the slope of the isotropic unloading line in the $\ln(1+e)$ vs. $\ln(p/p_r)$ space. φ_c is the critical state friction angle, which is for triaxial compression linked directly to the parameter M of the CC and 3SKH models through

$$\varphi_c = \sin^{-1} \left(\frac{6M}{3+M} \right) \quad (3)$$

The last parameter r determines the shear modulus, which for a given OCR depends linearly on the mean stress p , same as the bulk modulus does. Due to the non-linear character of the basic hypoplastic equation, the parameter r is usually calibrated by means of a parametric study, similarly to the parameter ψ of the 3SKH model.

4 Scalar error measure

In order to decrease the subjectivity of the model calibration and in order to assess the model performance in the pre-failure regime, a scalar measure of the "difference" between model predictions and experimental data has been introduced.

The suitable error measure should reflect differences in both predicted and observed stiffnesses and strain path directions. As experiments and simulations are characterised by identical stress paths, simulation error is here measured in the strain space. Let the pre-failure part of the stress path be subdivided into L increments, each of length $\Delta q = q_{max}/L$. Then, following Mašín et al. [14], the simulation error can be defined as

$$err(OCR, q_{max}) = \frac{\sum_{k=1}^L \left\| \Delta \epsilon_{sim}^{(k)} - \Delta \epsilon_{exp}^{(k)} \right\|}{\sum_{k=1}^L \left\| \Delta \epsilon_{exp}^{(k)} \right\|} \quad (4)$$

where $\Delta \epsilon_{exp}^{(k)}$ and $\Delta \epsilon_{sim}^{(k)}$ are the measured and predicted strain increment tensors, respectively, corresponding to the k -th stress increment of size Δq .

In order to demonstrate the meaning of the numerical value of err , it is plotted for two special cases in Fig. 3. First, experiment and simulation with identical strain path directions and different incremental stiffnesses (measured by their ratio $\alpha = \|\Delta \epsilon_{exp}^{(k)}\| / \|\Delta \epsilon_{sim}^{(k)}\|$ from (4), i.e. $\alpha = G_{sim}/G_{exp} = K_{sim}/K_{exp}$, where G and K are shear and bulk moduli respectively) are considered. In the second case experiment and simulation are characterised by identical incremental stiffnesses ($\alpha = 1$), but different directions of the strain paths measured by the angle ψ_ϵ in the Rendulic plane of ϵ (ϵ_a vs. $\sqrt{2}\epsilon_r$, where ϵ_a and ϵ_r are axial and radial strains respectively). Investigation of (4) reveals that $err = |1 - 1/\alpha|$ for the first case and $err = |2 \sin(\Delta\psi_\epsilon/2)|$ for the second one (with $\Delta\psi_\epsilon = \psi_{\epsilon sim} - \psi_{\epsilon exp}$).

Calculation of err is complicated by the scatter in experimental data, which becomes important in tests at low mean stresses p (high OCR s). Therefore, for calculating err the experimental data were approximated by smooth curves, namely by polynomial functions of the form

$$\epsilon_s = a_s q^{b_s} + c_s q^{d_s} + e_s q^{f_s} \dots \quad (5)$$

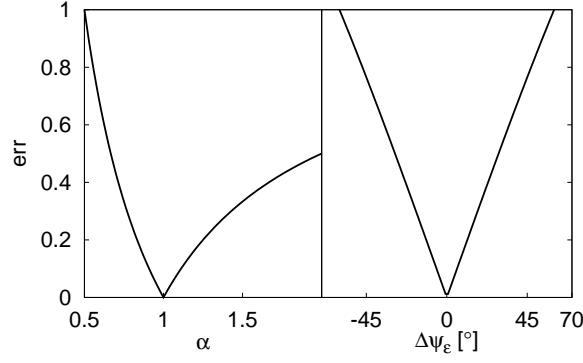


Figure 3: Numerical values of err for experiments and simulations that differ only in incremental stiffnesses (left) and strain path directions (right).

and

$$\epsilon_v = a_v q^{b_v} + c_v q^{d_v} + e_v q^{f_v} \dots \quad (6)$$

with coefficients $a_s, b_s, c_s, d_s, e_s, f_s \dots$ and $a_v, b_v, c_v, d_v, e_v, f_v \dots$. In this way a good fit of experimental data was achieved, as demonstrated in Fig. 4 for an experiment on kaolin clay with $OCR = 10$.

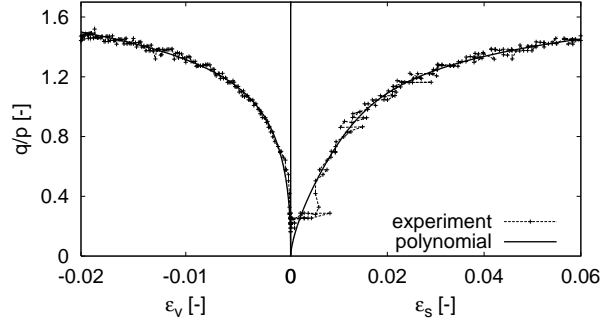


Figure 4: Approximation of experimental data on kaolin clay for $OCR = 10$ by a polynomial function for calculation of err .

In the present work, for all simulations q_{max} from Eq. (4) is chosen such that $q_{max} = 0.7q_{peak}$, where q_{peak} is the peak deviator stress achieved in the particular experiment. The value of err therefore corresponds to model prediction in the pre-peak, medium strain range, and thus its value should not be significantly influenced by localisation of deformation into shear bands. This occurred mainly in the tests on illitic clay at higher $OCRs$. L in Eq. (4) is taken high enough so it does not influence calculated err (typically, $L = 100$ was used).

5 Calibration

For the purpose of the calibration of the models we divide their parameters into two groups. In the first group are the parameters with a clear physical meaning, which are calibrated by standardized calibration procedures (e.g., φ_c, λ^*, N). The second group covers parameters whose calibration is rather subjective and they influence significantly the results of simulation of the shear tests, which are in a scope of this study (G, ψ, r). In the present work, parameters from the first group are calibrated using a standard procedures and their values are kept constant for all simulations. Parameters from the second group are found separately for different $OCRs$. In order to eliminate subjectivity from their calibration, they are evaluated by means of minimisation of the value of err from Eq. (4).

The initial states of p , q and e measured in the experiments were used in the simulations. In addition, the 3SKH model requires to specify the initial positions of the kinematic surfaces. These were aligned to reflect the stress history followed in the experiments (Fig. 5).

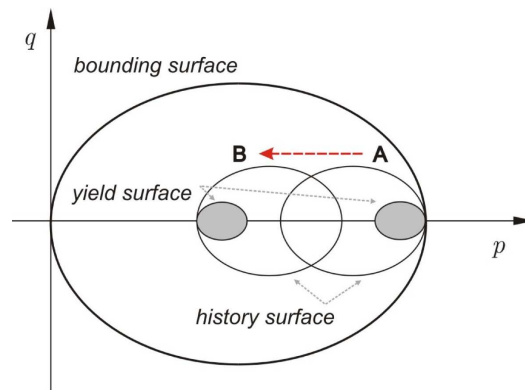


Figure 5: Sketch of the initial position of the kinematic surfaces of the 3SKH model for normally consolidated (A) and overconsolidated (B) states

5.1 The first group of parameters

Parameters N , λ^* and κ^* were found by evaluating an isotropic loading and unloading test, as demonstrated for the CC model in Fig. 6(a) for the kaolin clay and in Fig. 6(b) for the illitic clay. All isotropic experiments performed on illitic clay are shown in Fig. 6(b), which demonstrate consistent results for the slope λ^* and a certain scatter of the slope of the isotropic unloading line (parameter κ^*). Note that the numerical values of the parameter κ^* differ in Tab. 2, as they have slightly different physical interpretations in the three constitutive models. In the 3SKH model, κ^* specifies a bulk stiffness in the small strain range and it was calculated from an assumed Poisson ratio and the shear modulus, as accurate volumetric measurements in the small strain range were not available. In the HC model, the slope of the isotropic unloading line is for higher $OCRs$ influenced also by the non-linear character of the hypoplastic equation. For this reason, κ^* of the HC model could be considered to belong to the second group of parameters. However, as it has only minor effect on the predictions of shear tests (scope of this study), its value was kept constant for all simulations.

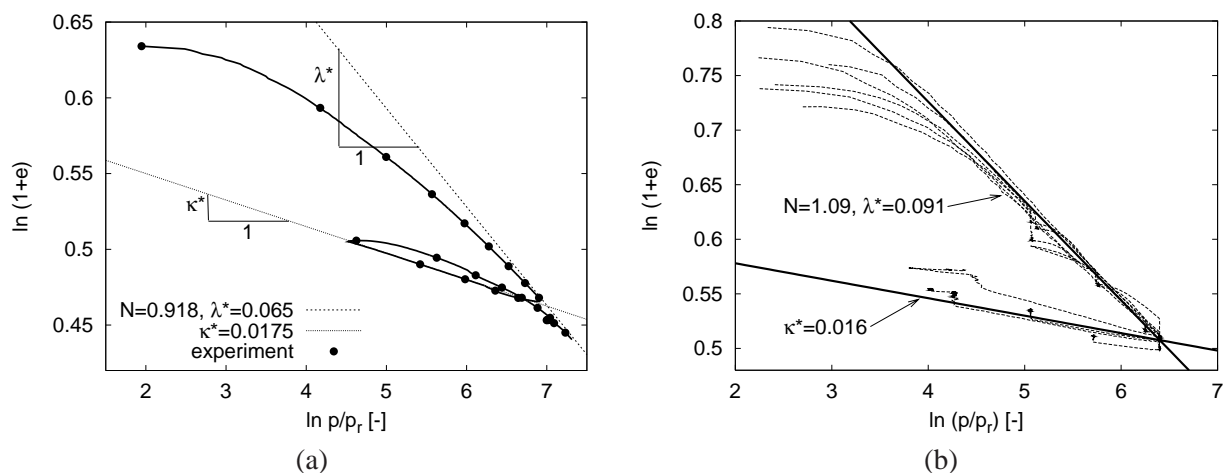


Figure 6: Calibration of parameters N , λ^* and κ^* of the CC model for kaolin clay (a) and illitic clay (b).

An approximate average value of the critical state friction angle from the shear experiments performed at

low $OCRs$ (so the results are not influenced significantly by localisation of deformation into shear bands) was used to calculate the parameters M and φ_c (linked via Eq. 3), see Fig. 7(a) for kaolin clay and Fig. 7(b) for the illitic clay.

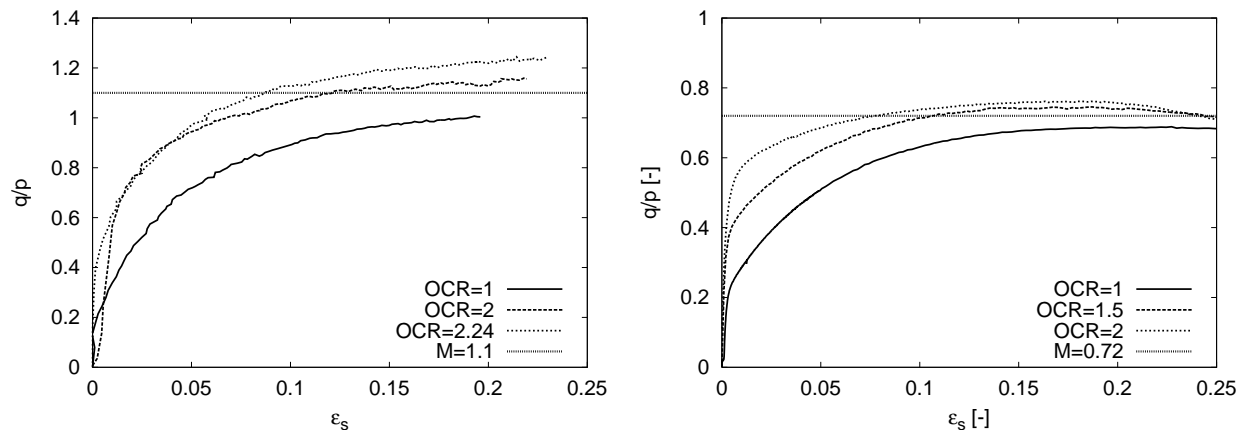


Figure 7: Calibration of parameter M (or, alternatively, φ_c) for kaolin clay (a) and illitic clay (b).

The 3SKH model requires five additional parameters that control the behaviour in the small strain range and the influence of the recent history (A , n , m , T and S). Neither the data on kaolin clay by Hattab and Hicher [6] nor the present data on illitic clay contain experiments required for their calibration. However, as these parameters do not influence significantly the results of the simulations in the medium strain range for tests with stress history shown in Fig. 5, they were taken over from different experimental studies on soils with similar mineralogy and granulometry as the soils used for the present evaluation. Namely, parameters evaluated using the tests on Speswhite kaolin by Stallebrass and Taylor [19] were considered relevant for the kaolin clay, and parameters evaluated by Mašín [10] using experiments on reconstituted and resedimented London clay [18] were considered representative for the illitic clay.

The parameters from the first group used in the present study are summarised in Table 1.

5.2 The second group of parameters

The parameters from the second group, namely G (CC), r (HC) and ψ (3SKH), influence significantly the results of the shear experiments in the pre-failure regime and their calibration is subjective. In order to eliminate this subjectivity, these parameters were found by minimizing the scalar error measure err defined in Sec. 4 (Eq. (4)). The calibration is demonstrated in the case of ψ of the 3SKH model using an experiment on kaolin clay at $OCR = 10$.

The relation between err and ψ is shown in Fig. 8. The curve has a clear minimum that corresponds to $\psi = 2.53$. To demonstrate the applicability of the proposed approach to calibration of the models, the optimised value of ψ , together with two different values, were used for simulation of the experiment, which was used for the calibration (Fig. 9). When both stress-strain diagram and the volumetric response in the pre-failure regime are taken into account, it may be concluded that the value of ψ found by optimisation with respect to err corresponds quite well to the value that could have been chosen by means of a subjective trial-and-error calibration procedure.

Parameters r and G were found using the same procedure as outlined above, a clear minimum of err was obtained in all cases. The only exception were tests on the illitic clay at low $OCRs$, where the change of the parameters leads to a gradual decrease of err without a minimum value.

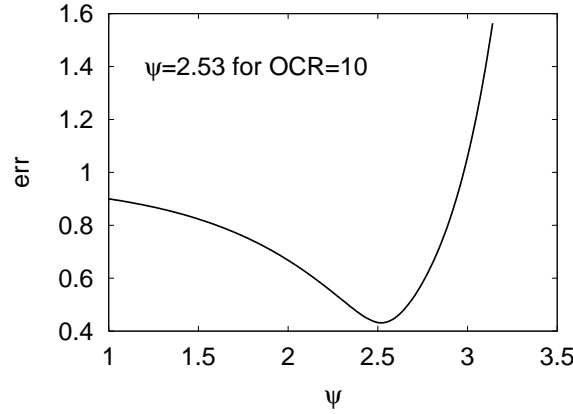


Figure 8: Calibration of ψ by means of minimisation of err for experiment on kaolin clay at $OCR = 10$.

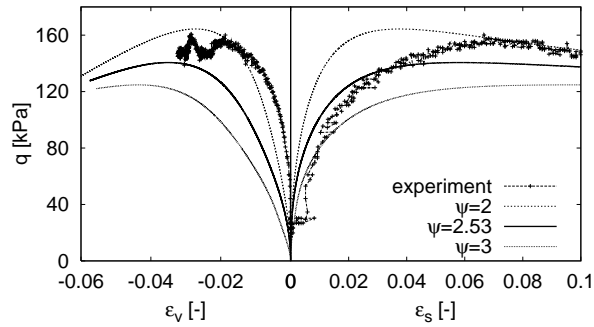


Figure 9: Predictions of the test on kaolin clay at $OCR = 10$ by the 3SKH model with err -optimised ($\psi = 2.53$) and two different values of ψ .

6 Performance of the models

6.1 Kaolin clay

The first insight into the performance of the models is provided by the graph where the values of the parameters from the second group calibrated by means of minimisation of err are plotted with respect to OCR . This graph is given in Fig. 10(a), the values of the parameters are normalised by their maximum values ($G_{max} = 9700$ kPa, $r_{max} = 1.43$, $\psi_{max} = 2.77$) so the results for the three models can be plotted in a single graph. Theoretically, if the models can quantitatively predict the behaviour of soils with different OCR s with a single set of material parameters, constant values of the parameters should be obtained.

For the CC model, Fig. 10(a) shows a clear trend of decreasing shear modulus G with increasing OCR . This is clearly consequence of the fact that in the simulated experiments the increasing OCR is linked to the decrease of the mean stress p ; no dependency of the parameter G on p is however assumed in the used version of the CC model. Assuming a dependency of G on p would lead to improvement of predictions. A clear trend in the dependency of the parameter ψ on OCR is observed for the 3SKH model. Unlike in the case of the CC model, however, the 3SKH model takes into account the influence of the mean stress. In this respect, predictions by the 3SKH model would be improved if a dependency of the parameter ψ on OCR was assumed. Last, the hypoplastic model requires high value of the parameter r for $OCR = 1$, and more-or-less constant values of r for higher OCR s. This suggests that the hypoplastic model should be calibrated separately for normally consolidated and overconsolidated states.

A quantitative response of the models is demonstrated in Fig. 10(b), where the value of the scalar error measure err is plotted with respect to OCR for "ideal" values of the parameters, i.e. the parameters that correspond to the minimum value of err (parameters from Fig. 10(a)). For these values of the parameters

the 3SKH model leads to the best predictions, followed by the hypoplastic and the CC model.

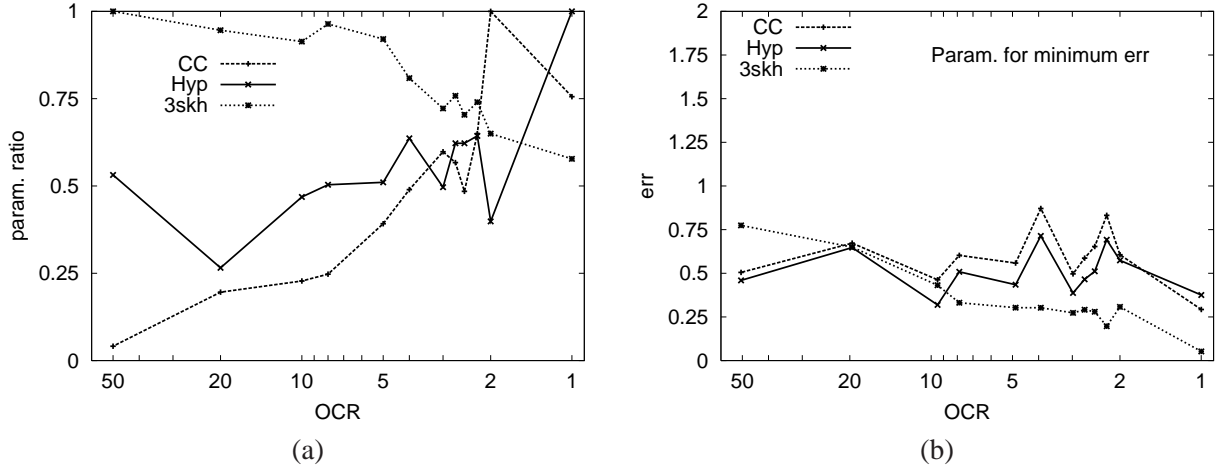


Figure 10: Parameters G , r and ψ normalised by their maximum values in a given set of simulations ($param. ratio$ is equal to G/G_{max} for CC model; r/r_{max} for hypoplastic model; ψ/ψ_{max} for the 3SKH model), calibrated using the err -minimisation procedure on kaolin clay (a). Values of err corresponding to optimised values of parameters (b).

In practical applications it is not possible to prescribe different values of material parameters, which lead to the highest possible accuracy, for each material element. Therefore Fig. 10 (b) is not fully representative of the actual model performance. For further evaluation of the performance of the models, the whole set of laboratory experiments has been simulated with two sets of material parameters, one optimised for normally consolidated states ($OCR = 1$) and one optimised for overconsolidated states ($OCR = 10$). The corresponding values of the parameters from the second group are in Tab. 2.

The relationship of err and OCR for the two cases is plotted in Fig. 11. As expected from the analysis of Fig. 10(a), for the parameters calibrated at $OCR = 1$ the hypoplastic model performs the worst (Fig. 11(a)). The two elasto-plastic models perform better, the err , however, in their case increase with OCR , because the difference of the actual and "ideal" values (Fig. 10(a) for $OCR = 1$) of the parameters progressively increase with increasing OCR . The advantage of the hypoplastic model is clear from Fig. 11(b), where the parameters were calibrated for $OCR = 10$. The prediction error of the hypoplastic model is smallest out of all models and does not depend substantially on OCR (even the error for $OCR = 1$ is relatively low, although it is obviously higher than its value from Fig. 11(a)). The prediction error of the elasto-plastic models increase with increasing difference between the actual OCR and $OCR = 10$. This demonstrates that the models are not capable of quantitatively correct predictions of tests at different OCR s with a single sets of material parameters. Assuming a dependency of their parameters on OCR as discussed in the paragraph related to Fig. 10(a) would, however, improve their predictions.

By definition, the value of err characterises the model predictions in the pre-failure regime only. In order to evaluate the predictions at failure, observed and predicted peak friction angles φ_p were plotted with respect to OCR . The results were similar for both sets of parameters, Fig. 12 shows them for the parameters optimised for $OCR = 10$. HC and 3SKH models predict the peak friction angles relatively accurately (HC is more accurate for $OCR \leq 10$, 3SKH for $OCR \geq 20$). CC model overestimates significantly φ_p for all states with $OCR > 2$. This is a well-known shortcoming of the CC model, caused by the elliptical shape of the yield surface.

While err gives a convenient quantitative measure of the model performance, it does not indicate the source of the prediction error. For qualitative comparison, the stress paths normalised by the Hvorslev equivalent pressure p_e^* are plotted for $OCR = 10$ optimised parameters in Fig. 13. The shape of the normalised stress paths is predicted relatively correctly by both the HC and 3SKH models, while overprediction of φ_p by the CC model is clear. All models, however, overestimate dilation. Normalised stress paths of all models head towards a unique critical state point, which has not been reached in the

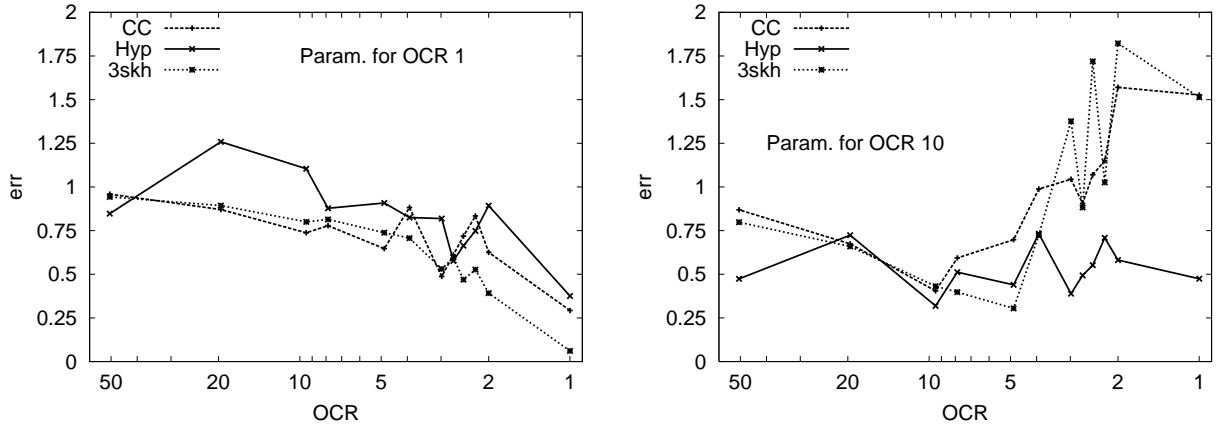


Figure 11: err for tests on kaolin clay, parameters optimised for $OCR = 1$ (a) and $OCR = 10$ (b).

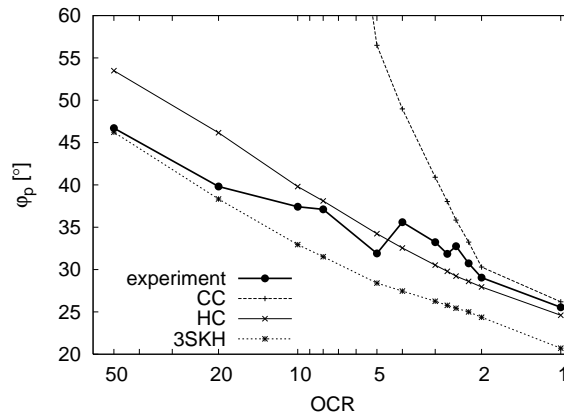


Figure 12: Peak friction angles φ_p for kaolin clay predicted by the models with parameters optimised for $OCR = 10$.

experiments at higher $OCRs$ (Fig. 13 top). A possible reason may be the localisation of deformation in shear bands at higher $OCRs$ despite using smooth platens and slenderness ratio of one in the triaxial tests.

Stress-strain curves for $OCR = 10$ optimised parameters are shown in Fig. 14(a). Low prediction errors by the HC model (Fig. 11) are reflected also in the qualitatively correct performance shown in Fig. 14(a). Qualitatively correct predictions with a gradual decrease of the shear stiffness are calculated also with the 3SKH model. The CC model due to the constant shear modulus G gives the worst predictions. The volumetric changes shown in Fig. 14(b) reveal a general trend of overestimation of dilation for higher $OCRs$, as already discussed in the previous paragraph. The CC model predicts an incorrect shape of the ϵ_v vs. ϵ_s curves, with no volumetric strains in the elastic range (caused by isotropic elasticity and $\dot{p} = 0$). The predictions by the two advanced models are in a much closer agreement with the experiments. A minor discrepancy of the 3SKH model is its prediction of dilatant behaviour immediately after the start of the shear phase for high $OCRs$. On the other hand, hypoplasticity overestimates the initial contraction for medium $OCRs$.

6.2 Illitic clay

The performance of the models with respect to experimental data on illitic clay will be studied in less detail, as lower number of experimental data is available to draw general conclusions. The same procedures have been applied as in the case of kaolin clay. The parameters have been optimised for $OCR = 1.5$ and $OCR = 8$, for their values see Tab. 2. The dependency of err on OCR for the two sets of parameters is shown in Fig. 15.

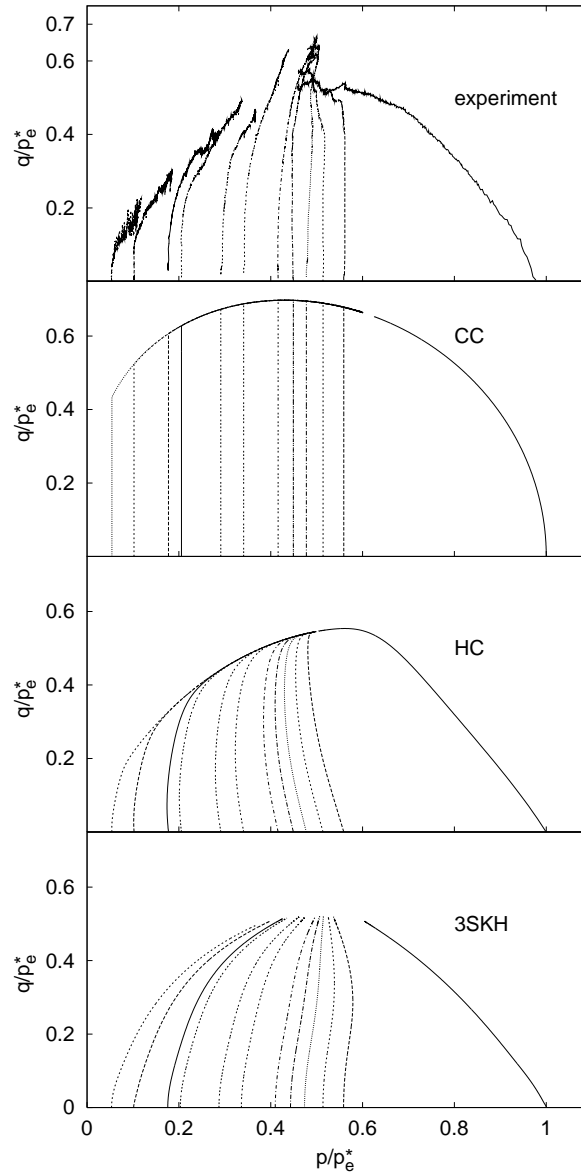


Figure 13: Stress paths normalised by p_e^* for $OCR = 10$ optimised parameters.

As in the case of the kaolin clay, the CC model gives the highest values of err . Conclusions for the hypoplastic model from the study on kaolin clay are confirmed. The values of the parameter r are similar for $OCR = 1.5$ and $OCR = 8$ and also the values of err are in both cases more-or-less constant for the whole range of $OCRs$. No significant difference in the calculated value of err is now observed for normally consolidated state. The value of err of the 3SKH model is significantly dependent on OCR . It gives the best predictions for $OCR \geq 4$, for $OCR \leq 2$ the values of err are smaller for the hypoplastic model.

From the qualitative point of view (Fig. 16) the results are again in agreement with the results on kaolin clay. The two advanced models give better predictions as they reproduce non-linearity of soil behaviour. For higher OCR the hypoplastic model predicts more significant initial volumetric contractancy than the 3SKH model, the experimental results are somewhat in between predictions by the 3SKH and hypoplastic models. The CC model gives qualitatively better predictions than the same model for tests on kaolin clay. This is due to the fact that the shortcomings of the CC model become more pronounced at high $OCRs$. The illitic clay was subjected to drained triaxial tests with constant cell pressure (as opposed to constant p tests on the kaolin clay), so the peak state was achieved at lower OCR than in the tests on kaolin clay.

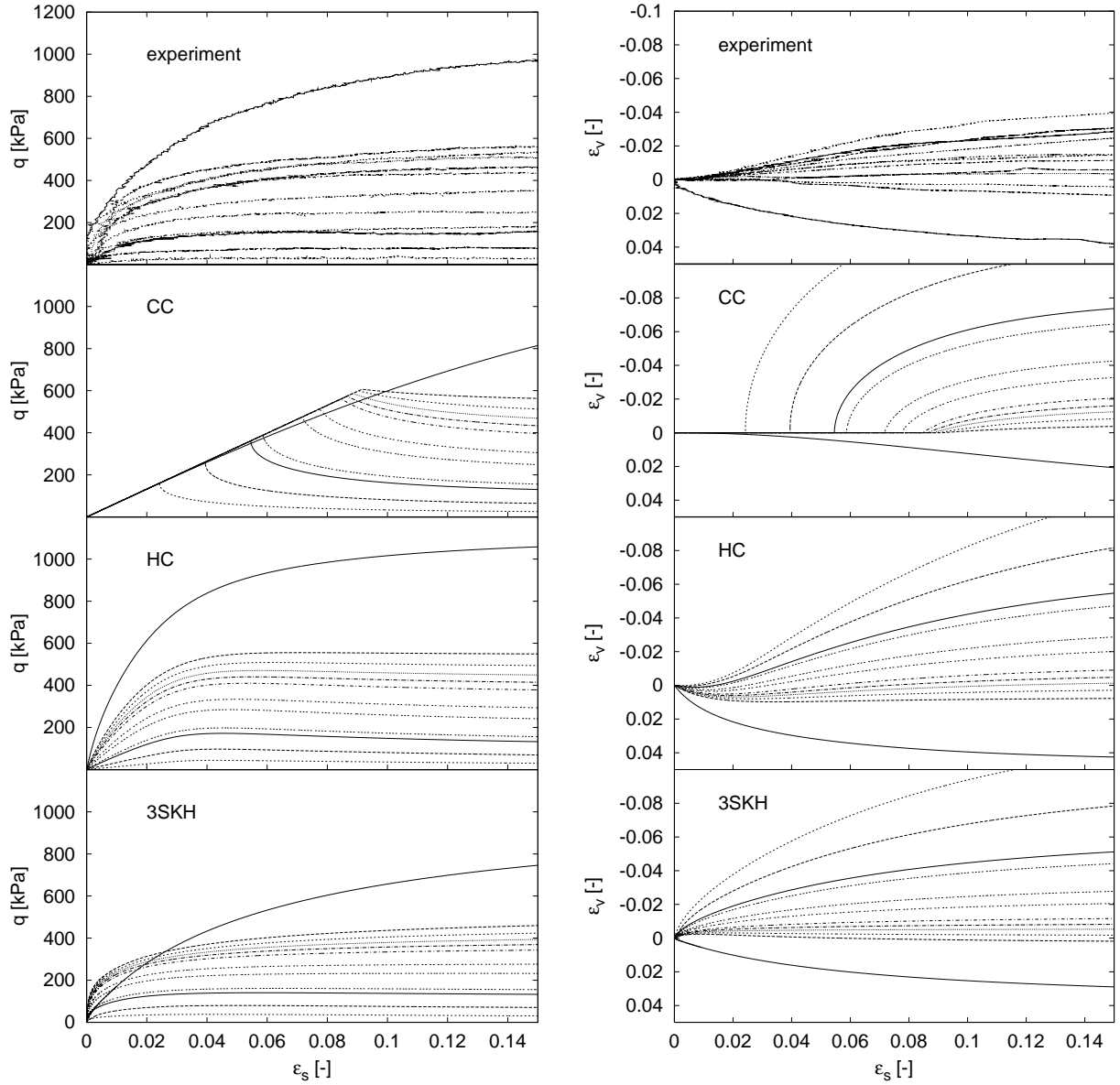


Figure 14: q vs. ϵ_s (a) and ϵ_v vs. ϵ_s (b) graphs for $OCR = 10$ optimised parameters on kaolin clay.

Tests at high initial OCR were not available for the illitic clay.

7 Limitations of the present work

In the presented evaluation we focus on a specific aspect of the predictive capabilities of the studied constitutive models - the influence of OCR at axisymmetric conditions with given stress path direction. The complete evaluation of the predictive capabilities of the models would require their testing under different orientations of stress paths in the stress space and at general 3D stress states. Such an evaluation has been presented elsewhere:

The first aspect, i.e. directional response, has been studied by Mašín et al. [14] who examined the same constitutive models as evaluated in the present Note. Using the concept of incremental strain response envelopes they have shown that unlike the CC model, the non-linear models (HC and $3SKH$) are capable of predicting correctly the dependency of incremental stiffness on the stress path direction.

The second aspect, i.e. response under general conditions, may be examined by simulations of real

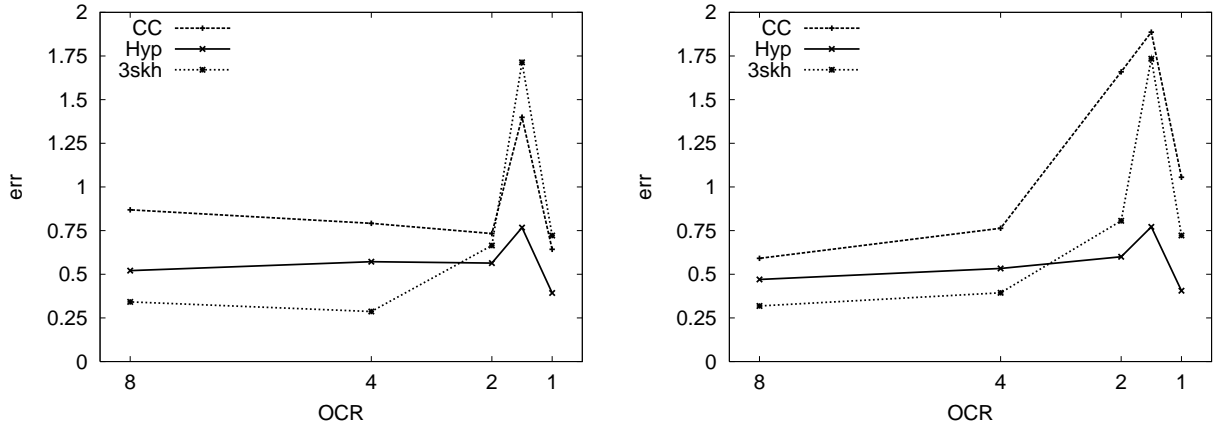


Figure 15: err for tests on the illitic clay, parameters optimised for $OCR = 1.5$ (a) and $OCR = 8$ (b).

boundary values problems. The three models from the present Note have been evaluated by the simulation of a tunneling problem in fine grained soils in Reference [12]. Advantages of the more advanced HC and 3SKH models when compared to the simpler CC model have clearly been demonstrated.

8 Conclusions

It has been demonstrated that the well-known shortcoming of the Modified Cam clay (CC) model, namely the elastic response inside the bounding surface (which coincides with the yield surface), is evident from both the qualitative comparison using the stress-strain diagrams and quantitative comparison using the scalar error measure err . The model gives, as expected, worse predictions than the two more advanced non-linear models. The predictions of the CC model would be improved if the shear modulus G was assumed to depend on the mean stress p (i.e., if constant poisson ratio ν was assumed instead of constant G).

The two advanced models (3SKH and HC) give qualitatively similar predictions, as both predict correctly the non-linear behaviour of overconsolidated soils. A single set of material parameters is sufficient for the hypoplastic model to predict the behaviour of soils with different $OCRs$ (except at the normally consolidated state) with approximately constant accuracy expressed in terms of the scalar error measure err . The model is therefore able to predict with a single set of parameters the change of soil behaviour with depth through the soil massive, which is desirable for practical applications. The simulation of normally consolidated kaolin clay suggests that the hypoplastic model should be calibrated separately for normally consolidated soil. This conclusion has, however, not been confirmed by evaluation of tests on illitic clay.

The performance of the 3SKH model for a single set of material parameters is less satisfactory in the sense that the prediction error err increases with increasing difference between the actual OCR and OCR for which the model has been calibrated. This observation should be taken into account in practical applications of the model, by assuming different values of ψ for different $OCRs$. Allowing for this dependency, predictions by the 3SKH model would be quantitatively better than predictions by the hypoplastic model.

In addition to evaluation of the model predictions in the pre-failure regime, predicted peak friction angles have been compared with the experimental results. As expected, the CC model significantly overpredicted φ_p at higher $OCRs$. This is a well-known shortcoming of the CC model imposed by the elliptical shape of the yield surface. Both advanced models gave satisfactory predictions, which were in a good agreement with the experimental data.

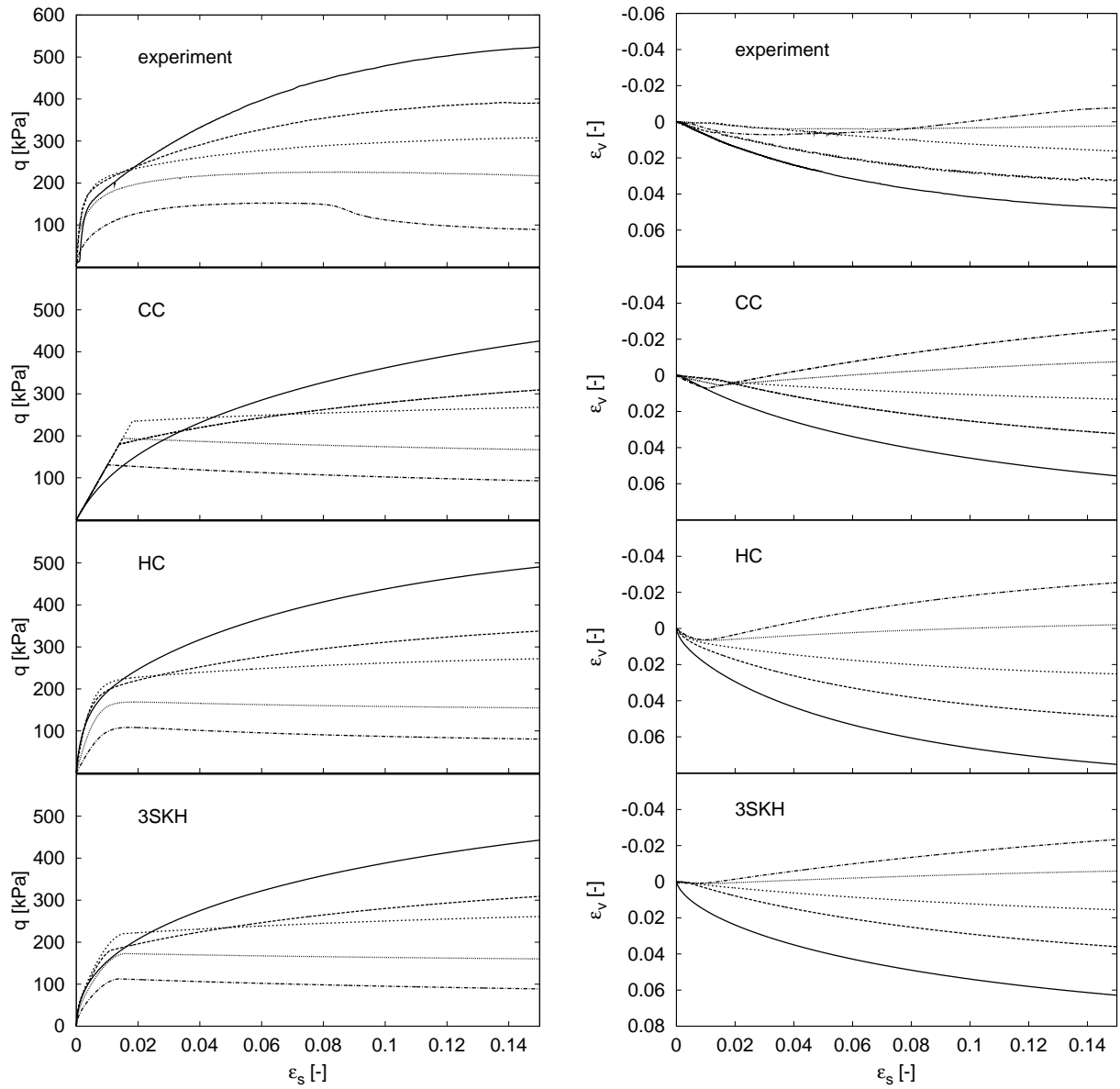


Figure 16: q vs. ϵ_s (a) and ϵ_v vs. ϵ_s (b) graphs for $OCR = 8$ optimised parameters on illitic clay.

9 Acknowledgement

The authors would like to thank to Prof. M. Hattab and Prof. P.-Y. Hicher, who kindly provided their experimental data on kaolin clay. The financial support by the research grants GAAV IAA200710605, MSM0021620855 and GAUK 6/2006/R is gratefully acknowledged.

References

- [1] A. Al Tabbaa and D. M. Wood. An experimentally based "bubble" model for clay. In *Proc. 3th Int. Conf. on Numerical Models in Geomechanics*. Niagara Falls, 1989.
- [2] J. H. Atkinson, D. Richardson, and S. E. Stallebrass. Effects of recent stress history on the stiffness of over-consolidated soil. *Géotechnique*, 40(4):531–540, 1990.
- [3] R. Butterfield. A natural compression law for soils. *Géotechnique*, 29(4):469–480, 1979.

- [4] G. Gudehus, A. Amorosi, A. Gens, I. Herle, D. Kolymbas, D. Mašín, D. Muir Wood, R. Nova, A. Niemunis, M. Pastor, C. Tamagnini, and G. Viggiani. The soilmodels.info project. *International Journal for Numerical and Analytical Methods in Geomechanics*, 32(12):1571–1572, 2008.
- [5] G. Gudehus and D. Mašín. Graphical representation of constitutive equations. *Géotechnique (in print)*, 2008.
- [6] M. Hattab and P.-Y. Hicher. Dilating behaviour of overconsolidated clay. *Soils and Foundations*, 44(4):27–40, 2004.
- [7] V. Herbstová, D. Mašín, and J. Boháč. Parameters for non-engineered colliery clayfills. In H. Bilsel and Z. Nalbantoglu, editors, *Proc. Int. Conf. on Problematic Soils (GEOPROB), Famagusta, Cyprus*, volume 1, pages 335–342. Eastern Mediterranean University Press, 2005.
- [8] I. Herle and D. Kolymbas. Hypoplasticity for soils with low friction angles. *Computers and Geotechnics*, 31(5):365–373, 2004.
- [9] D. Kolymbas. An outline of hypoplasticity. *Archive of Applied Mechanics*, 61:143–151, 1991.
- [10] D. Mašín. *Laboratory and Numerical Modelling of Natural Clays*. M. Phil. Thesis, City University, London, 2004.
- [11] D. Mašín. A hypoplastic constitutive model for clays. *International Journal for Numerical and Analytical Methods in Geomechanics*, 29(4):311–336, 2005.
- [12] D. Mašín. The influence of a constitutive model on predictions of a natm tunnel in stiff clays. In T. Triantafillidis, editor, *Proc. GKK 08 - Geomechanics Colloquium, Karlsruhe, Germany. Part 1 - Rock mechanics and Tunnelling*. University of Karlsruhe, 2008.
- [13] D. Mašín and I. Herle. State boundary surface of a hypoplastic model for clays. *Computers and Geotechnics*, 32(6):400–410, 2005.
- [14] D. Mašín, C. Tamagnini, G. Viggiani, and D. Costanzo. Directional response of a reconstituted fine grained soil. Part II: performance of different constitutive models. *International Journal for Numerical and Analytical Methods in Geomechanics*, 30(13):1303–1336, 2006.
- [15] Z. Mroz, V. A. Norris, and O. C. Zienkiewicz. An anisotropic hardening model for soils and its application to cyclic loading. *International Journal for Numerical and Analytical Methods in Geomechanics*, 2:203–221, 1978.
- [16] A. Niemunis. *Extended hypoplastic models for soils*. Habilitation thesis, Ruhr-University, Bochum, 2002.
- [17] K. H. Roscoe and J. B. Burland. On the generalised stress-strain behaviour of wet clay. In J. Heyman and F. A. Leckie, editors, *Engineering Plasticity*, pages 535–609. Cambridge: Cambridge University Press, 1968.
- [18] S. E. Stallebrass, J. H. Atkinson, and D. Mašín. Manufacture of samples of overconsolidated clay by laboratory sedimentation. *Géotechnique*, 52(2):249–253, 2007.
- [19] S. E. Stallebrass and R. N. Taylor. Prediction of ground movements in overconsolidated clay. *Géotechnique*, 47(2):235–253, 1997.
- [20] G. Viggiani and J. H. Atkinson. Stiffness of fine-grained soil at very small strains. *Géotechnique*, 45(2):245–265, 1995.
- [21] P. A. von Wolffersdorff. A hypoplastic relation for granular materials with a predefined limit state surface. *Mechanics of Cohesive-Frictional Materials*, 1:251–271, 1996.

List of Tables

1	Material parameters of the first group	16
2	Material parameters of the second group	16

Table 1: Material parameters of the first group

	kaolin clay				illitic clay					
	M, φ_c	λ^*	κ^*	N	M, φ_c	λ^*	κ^*	N		
CC	1.1	0.065	0.0175	0.918	0.72	0.091	0.016	1.09		
HC	27.5°	0.065	0.01	0.918	18.7°	0.091	0.01	1.09		
3SKH	1.1	0.065	0.0034	0.918	0.72	0.091	0.0084	1.09		
	A	n	m	T	S	A	n	m	T	S
3SKH	1964	0.65	0.2	0.25	0.08	457	0.71	0.27	0.24	0.16

Table 2: Material parameters of the second group

model (parameter)	kaolin clay		illitic clay	
	OCR 1	OCR 10	OCR 1.5	OCR 8
CC (param. G)	7330 kPa	2210 kPa	20000 kPa	4310 kPa
HC (param. r)	1.43	0.67	0.11	0.18
3SKH (param. ψ)	1.60	2.53	0.33	0.49

List of Figures

1	Stress paths of experiments used for evaluation of the models on kaolin clay by Hattab and Hicher [6] (a) and illitic clay (b).	2
2	Characteristic surfaces of the 3-SKH model, from Mašín et al. [14].	3
3	Numerical values of <i>err</i> for experiments and simulations that differ only in incremental stiffnesses (left) and strain path directions (right).	5
4	Approximation of experimental data on kaolin clay for $OCR = 10$ by a polynomial function for calculation of <i>err</i>	5
5	Sketch of the initial position of the kinematic surfaces of the 3SKH model for normally consolidated (A) and overconsolidated (B) states	6
6	Calibration of parameters N , λ^* and κ^* of the CC model for kaolin clay (a) and illitic clay (b).	6
7	Calibration of parameter M (or, alternatively, φ_c) for kaolin clay (a) and illitic clay (b).	7
8	Calibration of ψ by means of minimisation of <i>err</i> for experiment on kaolin clay at $OCR = 10$	8
9	Predictions of the test on kaolin clay at $OCR = 10$ by the 3SKH model with <i>err</i> -optimised ($\psi = 2.53$) and two different values of ψ	8
10	Parameters G , r and ψ normalised by their maximum values in a given set of simulations (<i>param. ratio</i> is equal to G/G_{max} for CC model; r/r_{max} for hypoplastic model; ψ/ψ_{max} for the 3SKH model), calibrated using the <i>err</i> -minimisation procedure on kaolin clay (a). Values of <i>err</i> corresponding to optimised values of parameters (b).	9
11	<i>err</i> for tests on kaolin clay, parameters optimised for $OCR = 1$ (a) and $OCR = 10$ (b).	10
12	Peak friction angles φ_p for kaolin clay predicted by the models with parameters optimised for $OCR = 10$	10
13	Stress paths normalised by p_e^* for $OCR = 10$ optimised parameters.	11
14	q vs. ϵ_s (a) and ϵ_v vs. ϵ_s (b) graphs for $OCR = 10$ optimised parameters on kaolin clay.	12
15	<i>err</i> for tests on the illitic clay, parameters optimised for $OCR = 1.5$ (a) and $OCR = 8$ (b).	13
16	q vs. ϵ_s (a) and ϵ_v vs. ϵ_s (b) graphs for $OCR = 8$ optimised parameters on illitic clay.	14